J Mol Model (2013) 19:5257–5266
DOI 10.1007/s00894-013-2020-8

ORIGINAL PAPER

Investigation of the binding network of IGF-I on the cavity surface of IGFBP4

Xin Chen · Shuyan Zhu · Danhui Duan · Tao Wu · Qi Wang

Received: 18 July 2013 / Accepted: 22 September 2013 / Published online: 17 October 2013

Abstract Insulin-like growth factor-binding proteins (IGFBPs) control bioactivity and distribution of insulin-like growth factors (IGFs) through high-affinity complex of IGFBP and IGF. To get more insight into the binding interaction of IGF system, the site-directed mutagenesis and force-driving desorption methods were employed to study the interaction mechanism of IGFBP4 and IGF-I by molecular dynamics (MD) simulation. In IGF-I, residues Gly7 to Asp12 were found to be the hot spots and they mainly anchored on the N-domain of IGFBP4. The contact area, the shape and size of protein, the surroundings of the binding site, the hydrophobic and electrostatic interaction between the two proteins worked as a complex network to regulate the protein-protein interaction. It was also found that the unfolding of the helix was not inevitable in the mutant, and it could be regulated by careful selection of the substituted amino acid.

Keywords Binding factors · Hot spots · IGFBP4-IGF-I · Interaction network · Mutation

Introduction

The insulin-like growth factor (IGF) system is a complex network which involves two IGF ligands (IGF-I and IGF-II), several cell surface receptors and six soluble high-affinity IGF binding proteins (IGFBP1-6) [1–3]. The IGFs bind to the receptors to activate their intrinsic tyrosine kinase domain activities. And then the activated receptors initiate the signaling cascades that ultimately result in the regulation of a number of biological responses. Simultaneously, the availability and bioactivity of IGF are modulated by the IGFBPs [4–6]. The ability of IGFBPs to bind IGF with high-affinity provides a latent IGF reservoir, and a rapid and controlled IGF release under certain physiological conditions is found to be performed. The growth promoting, differentiation and anti-apoptotic effects of IGFs are resulted from the interaction between the free IGF with the IGF receptors [7–10].

The interactions between IGF and IGFBPs have been extensively studied during the past decades, yet there is still little structural information from nuclear magnetic resonance (NMR) or crystallography spectroscopy available for the complexes. It has been found that the different binding specificities of IGF-I on IGFBP surface play a key role in the regulation of mitogenic and metabolic activities [11–13]. Then the structural characterizations of the molecular interaction between IGF and IGFBP are important for the understanding of the structural biology of IGF system. Alanine scanning mutagenesis is one of the most trendy methods for mapping the hot spots [14, 15]. However, it has also been found that the altered affinities are resulted not only in the removal of specific interactions through amino acid substitution but also in changing the global structure of IGF-I. Val11Ala, Asp12Ala, Gln15Ala and Phe16Ala were the key residues that were found to be important for the binding of IGF-I on IGF-1R. Yet the reduced α-helix content assessed by far-UV circular dichroism spectral analysis was proved to be involved in the binding surface of the two proteins. Therefore, the decreased binding affinities for these mutants may not accurately reflect the effect of removing the individual side chains but are most likely due to a local structural change [16]. Considering the two cooperative factors, the mutational analysis of IGF-I must take into account both functional and structural aspects to enable the interpretation of the binding residues.

X. Chen (✉) · S. Zhu · D. Duan
Institute of Environmental and Analytical Sciences,
College of Chemistry and Chemical Engineering, Henan University,
Kaifeng 475001, Henan, China
e-mail: xin_chen@henu.edu.cn

T. Wu · Q. Wang
Department of Chemistry, Zhejiang University,
Hangzhou 310027, Zhejiang, China

Steered molecular dynamics (SMD) method is an effective means to probe the mechanical properties of biomolecules and it has become a powerful tool for complementing in vitro single-molecule experiments [17–19]. The time-dependent external forces are applied to induce the unbinding of ligands and conformational changes in biomolecules on time scales accessible to molecular dynamics simulations. It has already provided important qualitative insights into biologically relevant problems for applications of the identification of ligand binding pathways [20–23]. For example, it has successfully revealed the participation of amino acid side groups in guiding biotin into its avidin binding site and the key binding residues involved in the adsorption of protein on biomaterials [20]. Then the binding sites of the IGF-I on IGFBPs could be defined by the SMD method.

While the structure of a complete IGFBP-IGF complex has not been solved, the entire and exact binding residues of the two proteins are still unclear. However, the structure of individual domains of IGFBP with IGF-I could provide segmental information to create a reasonable model for the IGFBP-IGF interaction. Sitar et al. [24] reported a crystal structure of a complex formed by IGFBP4 N-domain (Ala3–Leu82), IGFBP4 C-domain (Gly151–His229) and IGF-I (Pro2–Leu64). It has been found that the N-terminal region of IGFBP4 appears to wrap around IGF-I and forms contacts with residues Phe23, Tyr24 and Phe25. And the hole of IGFBP4 was filled by the N terminus of the IGF α-helix between Cys6 and Gly19 (i.e., Cys6, Gly7, Ala8, Glu9, and Leu10). Whereas the specific role of the individual residues involved in the interface with IGF-I and IGFBP4 were still not well identified. In this work, different kinds of site-directed mutations and force perturbation were applied to the system of IGF-I and IGFBP4 for mapping the binding determinants of the two proteins.

Materials and methods

System setup

The starting structure for the simulation of IGFBP4 and IGF-I was obtained from the protein data bank (PDB accession no. 2DSR) [24]. Missing hydrogen atoms were added using the AUTOPSF plug-in of VMD [25]. Missing residues were added with the I-TASSER server [26–28]. The purified proteins were solvated in a water box with the dimension of 59.9×69.3×141.9 $Å^3$. The system was composed of 55,100 atoms, and one sodium atom was added to neutralize the system.

Mutant preparation

Seven key binding residues (Gly7-Asp12) of IGF-I were determined in SMD simulation. Then six single-point mutant systems and five multi-point mutant systems were setup by VMD, respectively. As shown in Table 1, the single-point mutants were denoted as S1, S2, S3, S4, S5, and S6. And the multi-point mutants were named as M1, M2, M3, M4, and M5, respectively. The opposite polarity and the similar steric hindrance of the side chain of amino acid were the two mutational rules in this work. Then different kinds of substitutions were introduced in this work. And the original binding interaction could be weakened or broken by the substitution, and new binding interactions would be formed to change the binding state of IGF-I and IGFBP4. For example, the basic Glu9 was substituted by the neutral Leu9, and the negative charged $–COO^-$ was displaced by the isopropyl to remove the salt-bridge interaction between Glu9 and Lys223. As the carboxyl group was shown dominant binding ability in the wild-type (WT) system, the acidic Asp and Glu was set to be the preferred residues for the substitution of basic and neutral residues. The neutral Gly7, Ala8 and Val11 with small side chains were substituted by Asp. The neutral Leu10 was mutated by the basic Glu. The acidic Asp12 was substituted by Val to eliminate the original hydrogen bond (H-bond) interactions in the WT system. All the mutants were solved in water boxes with enough dimensions to accommodate the stretching of protein. Then energy minimization and molecular dynamics (MD) simulation were carried out for 10 ns to equilibrate the variants.

Molecular dynamics simulation

All the simulations in this work were performed with NAMD 2.7b [29] using Charmm27 [30] all-atom force field and the SPC model water molecules [31]. The integration timestep was 2 fs, and a cutoff of non-bonded van der Waals (VDW) force with a switching function starting at a distance of 10 Å. Long-ranged electrostatic interactions were calculated by the particle mesh Ewald (PME) summation. NPT ensemble was

Table 1 Substitution details of the single-point and the multi-point mutants

System	IGF-I mutant
S1	G7D
S2	A8D
S3	E9L
S4	L10E
S5	V11D
S6	D12V
M1	G7D, A8D
M2	G7D, A8D, E9L
M3	G7D, A8D, E9L, L10E
M4	G7D, A8D, E9L, L10E, V11D
M5	G7D, A8D, E9L, L10E, V11D, D12V

employed in MD simulations, and the temperature and pressure was kept constant at 310 K and 1 atm by Langevin method. Periodic boundary conditions were applied for MD simulations. Energy minimization was performed to optimize the geometry of protein and the solvated proteins were minimized by the steepest descent method. The parameters for the cross interactions were obtained from the Lorentz-Berthelot mixing rule. MD simulations of all the systems in this work were carried out for 10 ns.

Steered molecular dynamics simulation

SMD simulations for each system were carried out after the MD simulations. In order to detect the binding sites of IGFBP4 and IGF-I, the IGF-I was pulled away from the fixed IGFBP4 through constant pulling velocity (PCV) method. In PCV simulation, each Cα atom of IGF-I was attached to a dummy atom via a virtual spring. The dummy atom was moved at a constant velocity and then the force between the dummy atom and the Cα atom was measured using:

$$\vec{F} = -\nabla U \tag{1}$$

$$U = \frac{1}{2}k\left[vt - \left(\vec{r} - \vec{r}_0\right)\cdot\vec{n}\right]^2 \tag{2}$$

,where ∇U is the potential energy, k is the spring constant, v stands for pulling velocity, t means the time, $\vec{n}$ is the direction of pulling, $\vec{n}$ and $\vec{r}_0$ is the instantaneous position and the initial position of the Cα atom, respectively. The pulling direction was set to be along with the line of the mass center of IGFBP4 and IGF-I. To obtain the suitable observation window in SMD simulations of this work, a series of simulations on varied parameters were performed and the data were analyzed carefully in order to get the converged results. Finally, the spring constant k was set to be 30 kcal·mol^{-1}·Å^{-2} and the pulling velocity v was fixed at 5×10^{-4} Å·fs^{-1}. SMD simulations were introduced in the WT system and all 11 mutation systems to pull the IGF-I away from the IGFBP4. Each SMD simulation in this work was carried out for 125 ps to accommodate the total unbinding of IGF-I.

Analytical methods

Time evolutions of root mean square deviation (RMSD), potential energy, interaction energy, distances of binding couples and solvent accessible surface areas (SASA) during the simulations were calculated with the Timeline plug-in of VMD. The trajectories were also analyzed with VMD. The number of H-bonds and salt-bridge interactions on the interface were counted to get more insight into the molecular basis of the interaction between IGF-I and IGFBP4.

The contact area between IGFBP4 and IGF-I was calculated as:

$$A_{contact} = \frac{1}{2}\left(A_{IGFBP4} + A_{IGF-I} - A_{complex}\right) \tag{3}$$

where A_{IGFBP4} is the molecular surface area for IGFBP4, $A_{IGF\text{-}I}$ is the corresponding quantity for IGF-I, and A_{complex} is the surface area of the IGFBP4-IGF-I complex. The molecular surface area was defined as the solvent accessible surface area (SASA), which was calculated using the program VMD with the probe radius of 1.4 Å [32, 33].

Here the H-bond was defined by the following criterion: given a heteroatom A attached to an H-atom and another heteroatom B not bonded to A, an H-bond is formed only if the distance between two heavy atoms is smaller than 3.5 Å and the A-H-B angle is smaller than 30°.

For the salt-bridge interaction, the distance from the anionic carboxylate ($RCOO^-$) of either aspartic acid or glutamic acid and the cationic ammonium (RNH_3^+) from lysine or the guanidinium ($RNHC(NH_2)_2^+$) of arginine was defined. A distance cutoff of 4 Å was used as a discrimination criterion for the presence of salt-bridge.

The interaction energy (E_{inter}) was defined as:

$$E_{\text{inter}} = P_{IGFBP4} + P_{IGF-I} - P_{complex} \tag{4}$$

where E_{inter} is the total interaction energy between IGFBP4 and IGF-I, and P_{IGFBP4}, $P_{IGF\text{-}I}$, $P_{complex}$ are the potential energy of IGFBP4, IGF-I and the complex of IGFBP4 and IGF-I, respectively [34, 35].

Results and discussion

Screening of the hot spots

Protein-protein interaction is quite complex and it can be characterized by the shape, surface complementarity, flexibility of molecules, electrostatic and hydrophobic interactions [36–39]. The complex structure of IGFBP4 and IGF-I obtained from X-ray diffraction was stable and could be quickly equilibrated during the 10 ns MD simulation. As shown in Fig. 1, both the potential energy of the complex in water and the root mean square deviation (RMSD) of the backbone of the protein complex was shown to be fluctuated mildly around −1850 kcal·mol^{-1} and 1.95 Å, respectively. This showed that the complex has come to the equilibrium binding state. The X-ray diffraction structure of IGFBP4 and IGF-I was displayed in Fig. 2. It was discerned that the IGF-I was partly wrapped by the N-domain and C-domain of IGFBP4, and the cavity constructed by the two domains of IGFBP4 was just like a bowl to hold the IGF-I. Then most of the binding sites might be located at the inner surface of the IGFBP4 bowl.

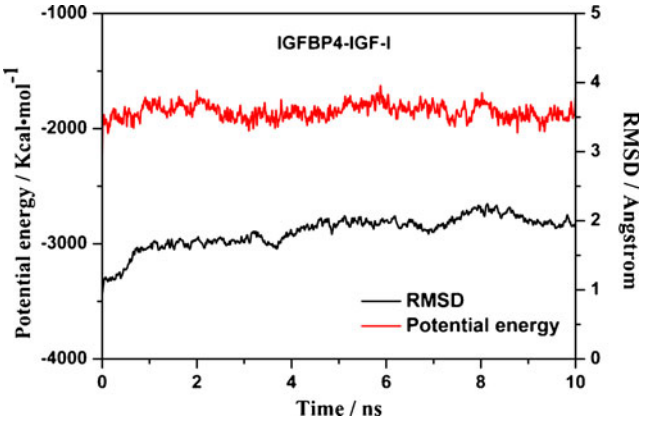

Fig. 1 The potential energy (red) and the RMSD (black) of the IGFBP4-IGF-I complex with respect to the MD simulation time

Following the MD simulation, the SMD simulation was performed on the equilibrated system. In order to clarify and specify the binding interface of the two proteins, the IGFBP4 was fixed and the backbone of IGF-I was pulled away. With the counteractive effect of the external force and the binding interaction, IGF-I desorbed from IGFBP4 in a stepwise manner. And the desorption snapshots were displayed in Fig. 3. IGF-I was composed of three α-helices and two short anti-parallel β-strands. It is shown in Fig. 2 that the helix was the primary secondary structure of IGF-I. Helix 1 (Gly7-Cys18) was just like a finger to insert into the IGFBP4 bowl and formed binding interaction. Whereas helix 2 (Ile43-Phe49) and helix 3 (Leu54-Met59) were located at the exterior of IGFBP4 bowl and no obvious binding sites were formed. It can be found from Fig. 3 that the exterior helices could be easily pulled away from the original location, however, the interior helix was difficult to be desorbed. The unfolding of helix 1 appeared in the SMD simulation, which was caused by the counterwork of the external force and the binding interaction of residues. One end of the helix was anchored at the inner surface of IGFBP4 bowl with the binding interaction, and it was strong enough to resist the external force for a long time. The helix was unfolded completely by the two opposite forces and then the binding interaction was completely broken by the external force. Therefore, it could be conclude that the binding interaction was larger than the H-bond interactions in α-helix. Then the key binding sites of IGFBP4 and IGF-I was discerned to be the residues located in the terminal of helix 1. It could also be clearly found in Fig. 4 that the complete desorption of IGF-I was associated with the unbinding of the tail residues in helix 1. Interaction energy between IGFBP4 and IGF-I in Fig. 4a was shown that the IGF-I was desorbed in a stepwise manner. The steps in the interaction energy curve were involved in the binding groups of the two proteins. And the last step was related with the binding group of helix 1, which was composed of the residues from Gly7 to Asp12. And it was consistent with the experimental data [24]. As the disulfide bond was formed between Cys6 and Cys48, the sequence from Gly7 to Asp12 was considered in this work. Comparing the distance of the six binding couples in Fig. 4b, it could be found that the original binding distances of Gly7, Glu9 and Asp12 were smaller than the other three binding couples. And the three residues play key roles on the binding of the complex of IGF-I and IGFBP4. Especially, the binding couple of Asp12:OD2 and Tyr49:HH was kept around 1.77 Å until 77.68 ps, which showed that Asp12 was the most important binding site of IGF-I.

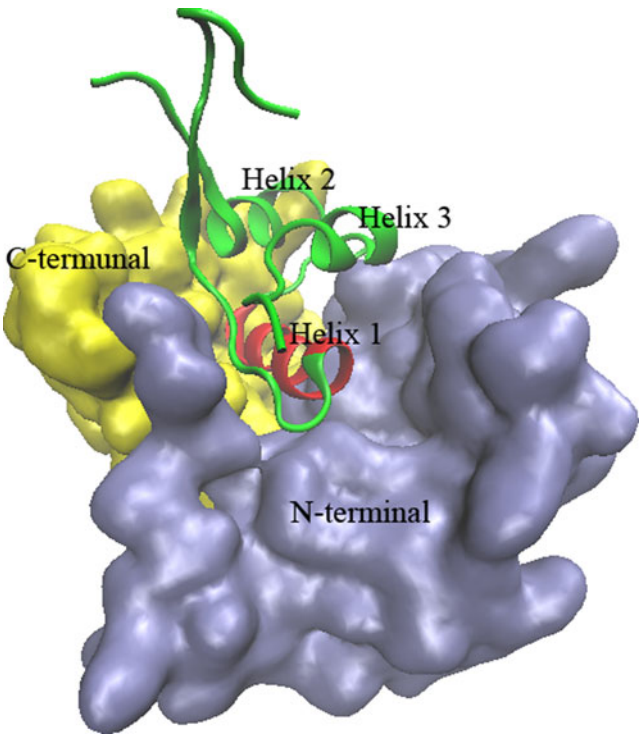

Fig. 2 Scheme of the X-ray diffraction structure of the N-terminal of IGFBP4 (purple), the C-terminal of IGFBP4 (yellow) and IGF-I (green and red). IGFBP4 was shown with surface model and IGF-I was displayed with cartoon model. Helix 1 of IGF-I which was inserted in the cavity of IGFBP4 was colored in red and the other part of IGF-I was colored in green

The binding information of IGF-I and IGFBP4 is listed in Table 2. As shown in this table, the binding couple was defined as the selected key residues of IGF-I and the binding residues of IGFBP4 within 5 Å of them. It could be found that the electrostatic interactions (H-bond and salt-bridge interactions) provided the major binding force, which appeared more than VDW interaction. It was discerned in the table that the hot spots of IGFBP4 were mainly located at the N-domain except for the Tyr49, which belongs to the C-domain. The acidic residues of Glu9 and Asp12 were shown to be the key binding residues of IGF-I, which formed many H-bond and salt-bridge interactions with the inner surface of IGFBP4. The carboxyl group was the key binding factor and readily formed electrostatic interaction with hydrogen atoms (ions). The $-COO^-$ group of Glu9 was close to the basic residues of Lys223

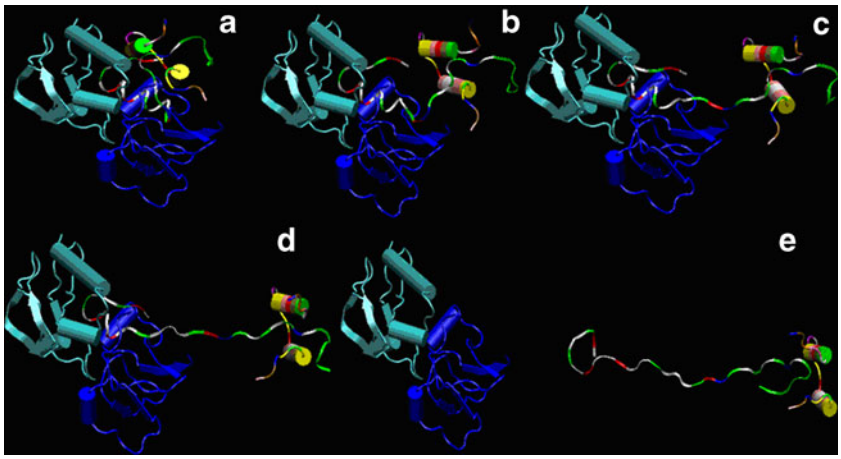

Fig. 3 Snapshots of the protein during the desorption process at (**a**) 0 ps, (**b**) 10 ps, (**c**) 40 ps, (**d**) 60 ps and (**e**) 125 ps in the WT system. The IGFBP4 C-terminal, the IGFBP4 N-terminal and the IGF-I were colored in blue, cyan and multicolor, respectively. Water molecules were not shown for clarity

and Arg202. Then both salt-bridge and H-bond interactions were formed in this binding region. H-bond interaction was also formed between the backbone –NH of Gly7 and Ala8 with the oxygen atom of IGFBP4. Whereas there no obvious electrostatic interaction appeared around Leu10 and Val11. As the two residues were close to the neutral Ile180 of IGFBP4, VDW interaction was the main driving force.

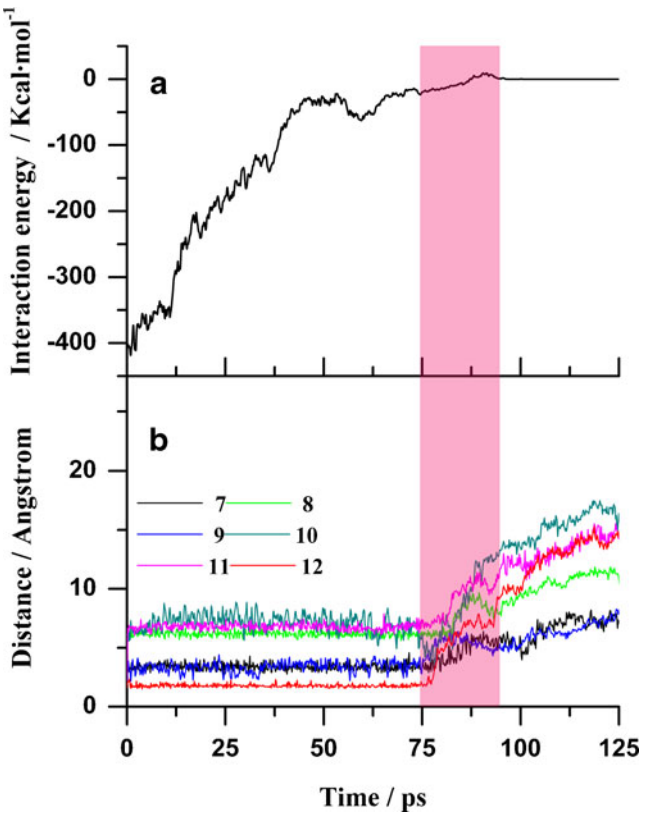

Fig. 4 (**a**) Interaction energy of IGFBP4 and IGF-I with respect to the SMD simulation; (**b**) The distance of the binding couple versus the SMD simulation time in the WT system. The numbers from 7 to 12 represented the binding couple of Gly7:HN-Pro180:O, Ala8:HN-Asn182:OD1, Glu9:OE2-Arg202:HH21, Leu10:HD11-Ile180:HD3, Val11:HG21-Leu175:HD1 and Asp12:OD2-Tyr49:HH, respectively

Single-point mutation scanning

As shown in Fig. 5, the order of the desorption time was S5> WT>S3>S2>S4>S1>S6. It was shown that the single-point mutation was not obviously effective in the decrease of the binding force between the two proteins. Except for S5, IGF-I was harder to be pulled away from the IGFBP4 than that in the WT system. Two kinds of mutation results were produced by

Table 2 Information of the binding couples of IGF-I and IGFBP4

	Binding couples		
IGF-I	IGFBP4	Distance	Binding type
Gly7-HN	Ile180-O (N-terminal)	4.29	H-bond
	Pro181-O(N-terminal)	3.87	H-bond
Ala8-HN	Asn182-OD1(N-terminal)	4.44	H-bond
	Cys194-O(N-terminal)	4.51	H-bond
Glu9-OE1	Lys223-HZ1(N-terminal)	4.14	SB
	Lys223-HZ2(N-terminal)	4.18	SB
	Lys223-HZ3(N-terminal)	2.91	SB
Glu9-OE2	Lys223-HZ1(N-terminal)	3.09	SB
	Lys223-HZ2(N-terminal)	3.38	SB
	Lys223-HZ3(N-terminal)	1.68	SB
	Arg202-HH11(N-terminal)	3.24	H-bond
	Arg202-HH21(N-terminal)	1.66	H-bond
	Arg202-HH22(N-terminal)	3.19	H-bond
Leu10-HD11	Ile180-HD3(N-terminal)	3.51	VDW
Val11-HG21	Ile180-HD2(N-terminal)	2.61	VDW
Asp12-OD1	Ala197-HN(N-terminal)	1.90	H-bond
Asp12-OD2	Tyr49-HH(C-terminal)	1.62	H-bond
	Ala197-HN(N-terminal)	2.37	H-bond

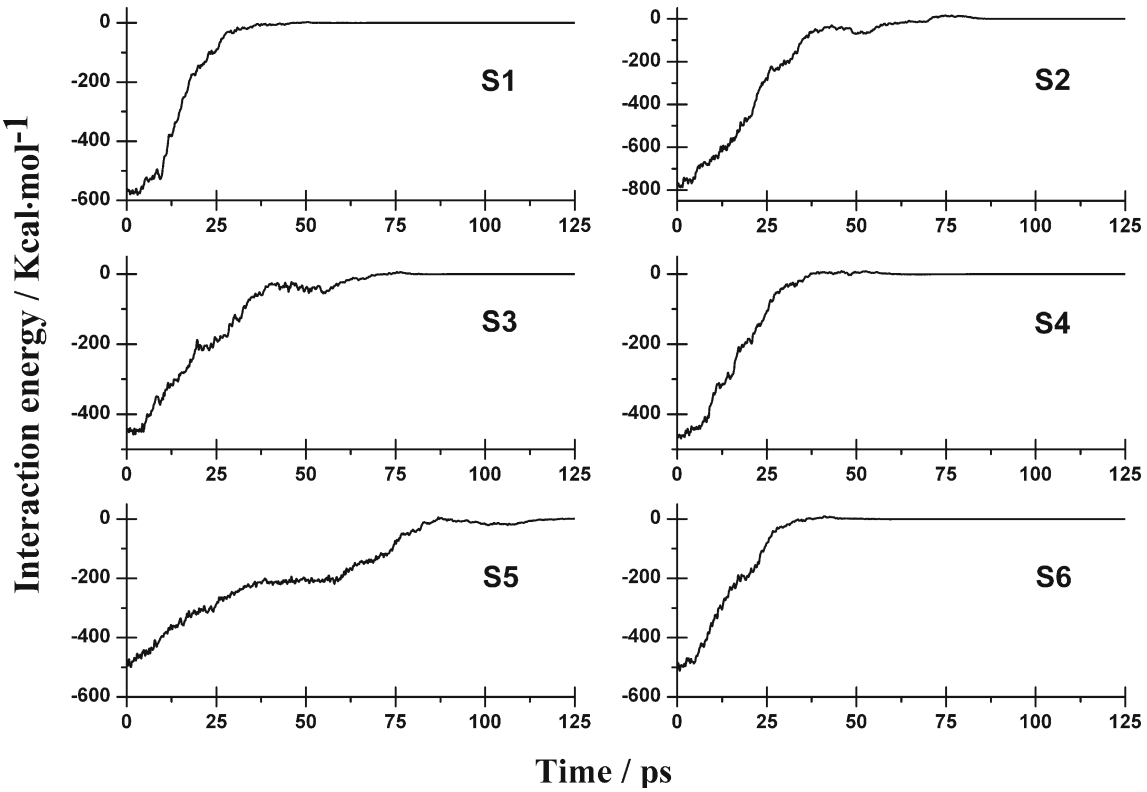

Fig. 5 Interaction energy between IGFBP4 and IGF-I in all six single-point mutation systems with respect to the SMD simulation time

the single-point mutation. The unfolding of helix 1 of IGF-I appeared in S2, S3 and S5 systems. Yet the IGF-I was pulled away from the IGFBP4 with the intact helix 1 in the S1, S4 and S6 systems. To get more insight into the binding interactions of IGFBP4 and IGF-I, the interaction energy (E_{inter}), the contact area ($A_{contact}$), the number of H-bond and salt-bridge (SB) on the interface of the two proteins, the complete desorption time ($t_{desorption}$) of IGF-I, the sequence identity of helix 1 in IGF-I at the equilibrium state (after MD simulation) and the unfolding state of helix 1 in IGF-I at the end of the SMD simulation of each system were listed in Table 3 (WT and single-point mutation systems) and Table 4 (multi-point mutation systems).

In company with the unfolding of helix 1, the desorption time of S2, S3 and S5 was shown to be larger than that of the other three mutant systems. New electrostatic interactions had been formed in these variants with the substitution. In S2 and S5 systems, the neutral residue was mutated by the acidic Asp. The carboxyl of Asp8 in S2 variant was found to form the H-bond interactions with $–NH_2$ of Asn182, which could enhance the binding interaction in this site. Furthermore, the steric hindrance of the substitution of A8D induced the conformation change of the binding region, which increased the contact area of IGFBP4 and IGF-I. Meanwhile the number of salt-bridges increased from 7 to 13, and the interaction energy between the two proteins was also increased 385.8 kcal·mol^{-1} to that of WT system. However, the number of H-bond was decreased from 16 to 11, and the unbinding of IGF-I in S2 system became easier than that in the WT system. And the S5 system with the substitution of V11D was found to show the enhancement of the binding interaction of IGFBP4 and IGF-I in the selected region. Further observation of the trajectory in the SMD simulation with VMD showed that helix 1 of IGF-I was also unfolded, which was the same for the WT system. As the space around Val11 was large enough to accept the substitution of Asp, then no obvious conformation change appeared in S5 mutant. Except for the original binding interaction between the two proteins, additional H-bond formed by Asp11 was shown to increase the binding ability of IGF-I on IGFBP4 surface. As shown in Table 3, there were no obvious differences of the interaction energy and the contact area between the WT and the S3 system. And the desorption time was reduced with the broken H-bonds and salt-bridges.

Asp was introduced in four mutation systems of S1, S2, S4 and S5. The acidic Asp was found to play the positive effect of the binding of IGFBP4 and IGF-I in S2 and S5 variants and to play the negative effect in S1 and S4 systems. For example, the carboxyl group of Asp7 in S1 was repulsed by the –C=O group of Ile180 and Pro181, which may accelerate the desorption of IGF-I. The shortest desorption time appeared with the substitution of Asp12 in S6 system. It can be found in Table 3 that the interaction energy, the contact area and the number of salt-bridge of S6 system was increased by 94.1 kcal·mol^{-1}, 59 Å^2 and 4, respectively. Yet the number of H-bonds was

Table 3 Binding information of the WT and the single-point mutation system

System	WT	S1	S2	S3	S4	S5	S6
E_{inter} (kcal·mol^{-1})	−407.3	−568.6	−793.1	−443.1	−456.6	−476.8	−501.4
$t_{desorption}$ (ps)	87.68	47.20	71.04	73.92	56.32	120.80	36.16
$A_{contact}$ (Å^2)	1419	1273	1671	1489	1231	1369	1478
H-bond number	16	19	11	11	9	12	14
SB number	7	7	13	5	4	8	11
α-helix sequence after MD	7-18	8-18	7-18	7-18	8-18	8-18	7-18
Unfolding of helix 1 after SMD	Y	N	Y	Y	N	Y	N

reduced from 16 to 14 and the desorption time was decreased by 51.52 ps, which showed that Asp12 was the primary hot spot of IGF-I.

Continuous multiple mutational analysis

The desorption time of the WT complex and the five multi-point variants was M3>M4>M2>M1>M5>WT. Then except for S5 system, all the IGF-I variants desorbed faster than the WT IGF-I. However, there no regular cumulative effect appeared in the multi-point mutation systems. In Fig. 6, it could be found that the converged time of the energy curves was various in the six systems. Especially in the M5 system, a notably sharp decrease of the interaction energy is observed. Rather than observing several steps in the WT system, here the interaction energy between the two proteins quickly comes to zero at 23 ps. Snapshots of the desorption process of the M5 system were displayed in Fig. 7. It was discerned in the graph that the IGF-I was easily pulled away from the IGFBP4 surface. And the three α-helices were all kept intact during the whole SMD simulation.

The conformational and structural change of the mutants was associated with the steric hindrance and the electrostatic interaction of the substituted amino acid. Resulted by the newly introduced side chain of the variant, the binding surface was redistributed with the re-accommodation of the conformation of protein. Then the binding state and desorption curve was diverse with the mutation. As shown in Table 4, helix 1 in all five mutants was kept intact after the SMD simulation. Yet helix 1 was partly unfolded in company with the multi-point mutation during the equilibrium MD simulation. For example, the sequence of helix 1 changed from Gly7-Cys18 to Glu10-Cys18 in M3 system. And two residues were also changed from the component of α-helix to the part of 3_{10}-helix in M4 system. In M5 system, all the values of the binding factors except for the interaction energy were smaller than that of the WT system, which was similar to the S6 system. The removal of Asp12 was shown to result in the decrease of the number of H-bonds and the fast desorption of IGF-I.

Network of the binding factors

To gain more direct insight into the relationship of the binding ability and the mutation, the binding factors listed in Tables 3 and 4 were plotted in Fig. 8. Two peaks appeared in the interaction energy curve, which belonged to the S2 and M1 variants, respectively. Interestingly, the two variants were both mutated with the substitution of A8D. Then the Asp8 in the variant was more likely to form stable interactions to stabilize the complex of IGFBP4 and IGF-I. Simultaneously, the surroundings of the binding site should be carefully considered. For example, there was no obvious energy increase occurred in the Asp-substituted system of S5. As the Asp7 was surrounded by the neutral residues in S5 variant, no electrostatic interaction was newly formed with the substitution. Then it was shown that the binding result was not only affected by the mutant residue, but also associated with the surroundings of the binding site.

Table 4 Binding information of the multi-point mutation system

System	M1	M2	M3	M4	M5
E_{inter} (kcal·mol^{-1})	−727.9	−684.5	−552.7	−552.4	−489.2
$t_{desorption}$ (ps)	63.52	67.20	85.68	67.52	23.00
$A_{contact}$ (Å^2)	1389	1474	1408	1438	1259
H-bond number	15	13	12	13	10
SB number	12	9	1	5	6
α-helix sequence after MD	7-18	7-18	10-18	9-18	7-18
Unfolding of helix 1 after SMD	N	N	N	N	N

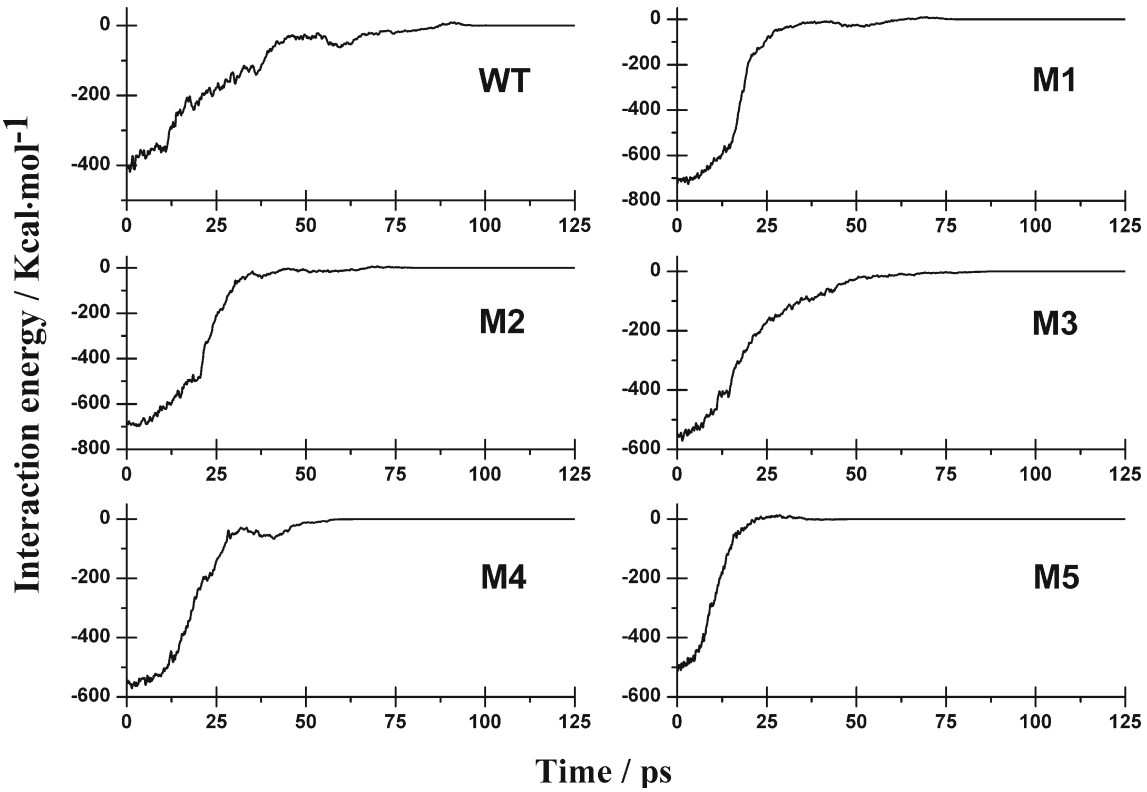

Fig. 6 Interaction energy between IGFBP4 and IGF-I in the WT system and the five multi-point mutation systems with respect to the SMD simulation time

For the analysis of H-bond, S1 variant was found to be the only system that formed more H-bonds on the interface of the two proteins than that of the WT system. Accordingly, the number of H-bond in M1 is the second peak in Fig. 8, which was resulted by the participation of Asp7. And the increase of the number of H-bond was also due to the electrostatic complementarity of IGF-I variant and IGFBP4.

The numbers of salt-bridge in S2 and M1 were the two notable peaks in the curve, which was similar to the interaction energy. And there are also two troughs of S4 and M3 in the graph, which are related with the mutation of L10E. When the Glu10 was substituted by the Leu10, the elimination of the acidic carboxyl group resulted in the breaking of salt-bridges. Accompanied with the unfolding of helix 1, only one salt-bridge remained in the M3 system.

In addition to the only obvious peak in S2 variant, the contact area was rather stable. The contact area of S2 was the largest one and it was larger than the WT system by 2.52 nm^2. By analyzing the structure of IGFBP4, it could be found that the space of the IGFBP4 bowl was large enough to

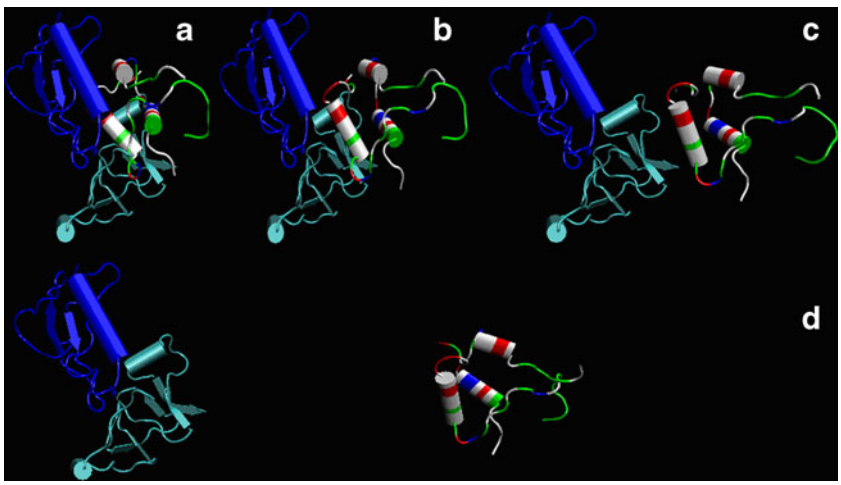

Fig. 7 Snapshots of the protein during the desorption process at (**a**) 0 ps, (**b**) 15 ps, (**c**) 23 ps and (**d**) 125 ps in the M5 system. The IGFBP4 C-terminal, the IGFBP4 N-terminal and the IGF-I were colored in blue, cyan and multicolor, respectively. Water molecules were not shown for clarity

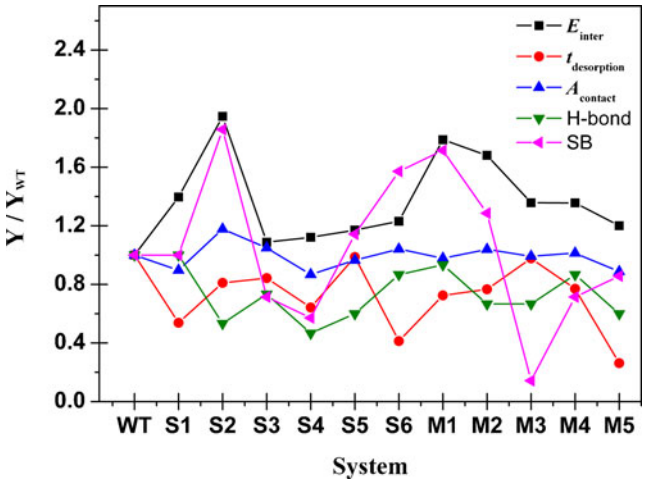

Fig. 8 The relative value of the interaction energy (E_{inter}), the desorption time ($t_{desorption}$), the contact area ($A_{contact}$), the number of H-bond and the number of salt-bridge (SB) of all the systems. The value of WT was defined as a reference value

accommodate the structural change of IGF-I. Thereby, there was no obvious change of the contact area in all the systems.

S5 variant was the only mutation that produced a longer desorption time than the WT system. The desorption time of S1, S6 and M5 was the notable points in the desorption time curve. The faster desorption of IGF-I in S6 and M5 systems were associated with the substitution of Asp12, and the fast unbinding of IGF-I in the S1 system was resulted by the substitution of G7D.

It can be found from Fig. 8 that the fluctuation trend of H-bond and salt-bridge was consistent with that of interaction energy, which showed that the interaction energy of IGFBP4 and IGF-I was mainly associated with the formation of H-bond and salt-bridge. However, the curve shapes of all the binding factors were not uniform. For example, the substitution in S2 variant resulted in the increase of contact area, interaction energy and the number of H-bonds between the two proteins. Yet the desorption time of the S2 system became shorter than that of the WT system.

Among all six single-point mutation systems, it could be found that the desorption time was notably decreased by the mutation in the S1 and S6 systems. In these two systems, the helix structure was kept intact after the mutation. Yet the desorption mechanism of the IGF-I variant in the two systems was different. In the S1 system, the carboxyl of the new Asp7 was repulsed by the carbonyl of Ile170 on the surface of IGFBP4. Whereas the substitution of Asp12 by Leu12 in the S6 system was found to result in the removal of the original electrostatic interactions, and then the desorption of IGF-I became easier.

It was found that the unfolding of the helix was not inevitable for the mutation. The unfolding of helix 1 resulted by the mutation that occurred in the IGF-I mutants of S1, S4, S5, M3 and M4 systems. Only one residue was found to be unfolded from the α-helix in the single-point mutant, whereas three and two residues were found to be lost from helix 1 in the multi-point mutants of M3 and M4, respectively. All the unfolding of helix 1 began from residue 33, which was the terminus of the helix.

Therefore, it could be concluded that the binding of IGF-I on IGFBP4 was affected by many interdependent binding factors, such as the interaction energy, the contact area, the structure of protein, the number and the type of the interaction between the two proteins. They worked together to form a complex network.

Conclusions

By performing the MD simulation of site-directed mutagenesis and the force-driving desorption on the WT, the single-point mutation and the multi-point mutation systems of the IGFBP4-IGF-I complex, the interactive binding network of proteins was discussed in this work. Different from the common ala-scanning mutagenesis, substitution by residues of the anti-polar side chains was employed in this work. The inner cavity of IGFBP4 was just like a bowl to wrap the helix finger of IGF-I, and it was large enough to adapt the structural adjustment of IGF-I. The shape and size complementarity provided the prerequisite for IGF-I binding on IGFBP4. Residues Gly7 to Asp12 of IGF-I were found to be hot spots on the binding interface, and they mainly bonded to the N-domains of IGFBP4. The H-bond and the salt-bridge interactions were driving forces to stabilize the complex of IGFBP4 and IGF-I. It was also found that the reduction of the helix content was not inevitable for the mutants, and then the amino acid scanning mutagenesis could be regulated to be applied for specifying the single binding residue. By comparing the single-point and the multi-point mutations, it was found that no obvious cumulative effect appeared with the increase of the mutant site. Especially, the force-driving desorption result was shown to be directly associated with the key binding residues. And it could classify the binding residues with the single-point mutagenesis. The complex of IGF-I and IGFBP4 was shown to be a typical model to study the protein-protein interaction. The interdependent binding factors discussed above formed a network and worked together on the binding interaction of IGF-I and IGFBP4, which might provide more insight into the interaction mechanism of protein-protein system and be helpful for the structure based drug design.

Acknowledgments This work was financially supported by the National Natural Science Foundation of China (Grant No. 21003037 and No. 30900236) and the National Science Foundation of the Education Department of Henan Province (13A150085).

Reference

1. Jones JI, Clemmons DR (1995) Endocr Rev 16:3–34
2. Holly J, Perks C (2006) Neuroendocrinology 83:154–160
3. Hwa V, Oh Y, Rosenfeld RG (1999) Endocr Rev 20:761–787
4. Denley A, Cosgrove LJ, Booker GW, Wallace JC, Forbes BE (2005) Cytokine Growth Factor Rev 16:421–439
5. Collett-Solberg PF, Cohen P (2000) Endocrine 12:121–136
6. Gonzalez C, Auw Yang KG, Schwab JH, Fitzsimmons JS, Reinholz MM, Resch ZT, Bale LK, Clemens VR, Conover CA, O'Driscoll SW, Reinholz GG (2010) Growth Horm IGF Res 20:81–86
7. Carrick FE, Wallace JC, Forbes BE (2002) Lett Protein Sci 8:147–153
8. Baxter RC, Meka S, Firth SM (2002) J Clin Endocr Metab 87:271–276
9. Baxter RC (2000) Am J Physiol Endoc M 278:E967–E976
10. Stewart CE, Rotwein P (1996) Physiol Rev 76:1005–1026
11. Bach LA, Hsieh S, Sakano K, Fujiwara H, Perdue JF, Rechler MM (1993) J Biol Chem 268:9246–9254
12. Ning Y, Schuller AGP, Conover CA, Pintar JE (2008) Mol Endocrinol 22:1213–1225
13. Collett-Solberg PF, Cohen P (1996) Endocrinol Metab Clin North Am 25:591–614
14. Dubaquié Y, Lowman HB (1999) Biochemistry 38:6386–6396
15. Simonsen SM, Sando L, Rosengren KJ, Wang CK, Colgrave ML, Daly NL, Craik DJ (2008) J Biol Chem 283:9805–9813
16. Jansson M, Uhlen M, Nilsson B (1997) Biochemistry 36:4108–4117
17. Sotomayor M, Schulten K (2007) Science 316:1144–1148
18. Marszalek PE, Lu H, Li H, Carrion-Vazquez M, Oberhauser AF, Schulten K, Fernandez JM (1999) Nature 402:100–103
19. Isralewitz B, Baudry J, Gullingsrud J, Kosztin D, Schulten K (2001) J Mol Graph Model 19:13–25
20. Izrailev S, Stepaniants S, Balsera M, Oono Y, Schulten K (1997) Biophys J 72:1568–1581
21. Wriggers W, Schulten K (1999) Proteins 35:262–273
22. Skovstrup S, David L, Taboureau O, Jørgensen FS (2012) PLOS ONE 7:e39360
23. Le L, Lee EH, Hardy DJ, Truong TN, Schulten K (2010) PLOS Comput Biol 6:e1000939
24. Sitar T, Popowicz GM, Siwanowicz I, Huber R, Holak TA (2006) Proc Natl Acad Sci U S A 103:13028–13033
25. Humphrey W, Dalke A, Schulten K (1996) J Mol Graphics 14:33–38
26. Zhang Y (2008) BMC Bioinforma 9:40–47
27. Roy A, Kucukural A, Zhang Y (2010) Nat Protoc 5:725–738
28. Roy A, Yang J, Zhang Y (2012) Nucleic Acids Res 40: W471–W477
29. Kale L, Skeel R, Bhandarkar M, Brunner R, Gursoy A, Krawetz N, Phillips J, Shinozaki A, Varadarajan K, Schulten K (1999) J Comput Phys 151:283–312
30. MacKerell AD, Bashford D, Bellott, Dunbrack RL, Evanseck JD, Field MJ, Fischer S, Gao J, Guo H, Ha S, Joseph-McCarthy D, Kuchnir L, Kuczera K, Lau FTK, Mattos C, Michnick S, Ngo T, Nguyen DT, Prodhom B, Reiher WE, Roux B, Schlenkrich M, Smith JC, Stote R, Straub J, Watanabe M, Wiórkiewicz-Kuczera J, Yin D, Karplus M (1998) J Phys Chem B 102:3586–3616
31. Zielkiewicz J (2005) J Chem Phys 123:104501–104506
32. Chiu C, Dieckmann GR, Nielsen SO (2008) J Phys Chem B 112: 16326–16333
33. Ortiz V, Nielsen SO, Klein ML, Discher DE (2005) J Mol Biol 349: 638–647
34. Chen X, Wu T, Wang Q, Shen JW (2008) Biomaterials 29:2423–2432
35. Shen JW, Wu T, Wang Q, Pan HH (2008) Biomaterials 29: 513–532
36. Jones S, Thornton JM (1996) Proc Natl Acad Sci U S A 93:13–20
37. Tsai CJ, Nussinov R (1997) Protein Sci 6:1426–1437
38. Fernandez A, Scheraga HA (2003) Proc Natl Acad Sci U S A 100: 113–118
39. Moreira IS, Fernandes PA, Ramos MJ (2007) Proteins 68:803–812